Northumbria Research Link

www.northumbria.ac.uk/nrl

northumbria
UNIVERSITY
University Library

Vibration analysis of thin-walled composite beams with I-shaped cross-sections

Thuc Phuong Vo* and Jaehong Lee†

Department of Architectural Engineering, Sejong University
98 Kunja Dong, Kwangjin Ku, Seoul 143-747, Korea

(Dated: July 6, 2010)

A general analytical model applicable to the vibration analysis of thin-walled composite I-beams with arbitrary lay-ups is developed. Based on the classical lamination theory, this model has been applied to the investigation of load-frequency interaction curves of thin-walled composite beams under various loads. The governing differential equations are derived from the Hamilton's principle. A finite element model with seven degrees of freedoms per node is developed to solve the problem. Numerical results are obtained for thin-walled composite I-beams under uniformly distributed load, combined axial force and bending loads. The effects of fiber orientation, location of applied load, and types of loads on the natural frequencies and load-frequency interaction curves as well as vibration mode shapes are parametrically studied.

_____

*Postdoctoral research fellow

†Professor, corresponding author. Tel.:+82-2-3408-3287; fax:+82-2-3408-3331

; Electronic address: `jhlee@sejong.ac.kr`

NOMENCLATURE

A	Cross section area
$\bar{a}$	Location of transverse load with respect to shear center
b_1, b_3	Width and height of I-section
E_{ij}	Stiffness coefficients of thin-walled composite beams
E_1, E_2	Young's moduli in the 1- and 2-directions of lamina
$(EA)_{com}$	Axial rigidity of composite beam
$(EI_x)_{com}, (EI_y)_{com}$	Flexural rigidity with respect to x- and y-axis
$(EI_\omega)_{com}$	Warping rigidity
$f(z), g(z)$	Polynomial functions which depend on the loading pattern
G_{12}	Shear moduli in the 1-2 plane of lamina
$(GJ)_{com}$	Torsional rigidity
I_p	Polar moment of inertia about the centroid
$[K], [G_1], [G_2], [M]$	Stiffness, geometric and mass matrix in finite element formulation
m_0, m_c, m_p, m_s, m_2	Inertia coefficients
M_b	External uniform bending moment
M_{cr_n}	Buckling moments for pure bending
M_t	Torsional moment
M_x, M_y	Bending moments with respect to x- and y-axis
M_ω	Warping moment
$\overline{M}_{cr}, \overline{M}_{x_n}$	Nondimensional bending moment
N_0	External axial force
N_z	Axial force
p	Transverse load
$P_{x_n}, P_{y_n}, P_{\theta_n}$	Flexural buckling loads in the x- and y-axis and torsional buckling load
$\overline{P}_{cr}$	Nondimensional vertical concentrated load
$\overline{P}_{x_n}, \overline{P}_{y_n}, \overline{P}_{\theta_n}, \overline{N}_{cr}$	Nondimensional axial force
q, r	Coordinate of point on the contour in the (n, s) coordinate system
$\overline{q}_{cr}$	Nondimensional uniformly distributed load
$(\bar{Q}_{ij}^*)^k$	Transformed reduced stiffness of the kth lamina
t	Flange and web thickness of I-section

1	$\mathcal{T}, \mathcal{U}, \mathcal{V}$	Kinetic energy, strain energy and potential energy
	u, v, w	Displacements of a point on the contour in the (n, s, z) coordinate system
	U, V, W	Displacement components of the pole in the (x, y, z) coordinate system
	$\bar{u}, \bar{v}, \bar{w}$	Midsurface displacements of a point on the contour in the (s, z) coordinate system
	x_p, y_p	Coordinates of pole in the (x, y) coordinate system
	α	Angle between x and tangent axis
	$\{\Delta\}$	Eigenvector of nodal displacements corresponding to an eigenvalue
	$\epsilon_z, \epsilon_z^\circ, \bar{\epsilon}_z$	Axial strain in the (n, s, z) coordinate system
	θ	Fiber orientation
	κ_x, κ_y	Curvatures with respect to the x- and y-axis
	$\kappa_{sz}, \kappa_\omega$	Twisting and warping curvature
	$\bar{\kappa}_{sz}, \bar{\kappa}_z$	Midsurface curvatures
	λ	Buckling parameter
	ν_{12}	Poissons ratio
	Π	Total potential energy
	ρ	Density of composite material
	σ_z, γ_{sz}	Normal and shear stresses in the (n, s, z) coordinate system
	Φ	Angle of rotation of the cross section about the pole axis
	Ψ_j, ψ_j	Interpolation function in finite element formulation
	$\omega(s)$	Warping function
	$\omega_{x_n}, \omega_{y_n}, \omega_{\theta_n}$	Flexural natural frequencies with respect to the x- and y-axis and torsional natural frequencies
	$\omega_{xx_n}, \omega_{ya_n}, \omega_{yb_n}$	Natural frequencies for simply supported composite beams under axial force and uniform bending
	$\overline{\omega}$	Nondimentional natural frequency

1. INTRODUCTION

Fiber-reinforced composite materials have been used over the past few decades in a variety of structures. Composites

have many desirable characteristics, such as high ratio of stiffness and strength to weight, corrosion resistance and

magnetic transparency. Thin-walled structural shapes made up of composite materials, which are usually produced

by pultrusion, are being increasingly used in many civil, mechanical and aerospace engineering applications.

Up to the present, investigation into the vibration and stability analysis of thin-walled members has received widespread attention and has been carried out extensively since the early works of Vlasov [1], Gjelsvik [2]. It is also well known that the vibration behavior of these members under various loads display complex response. Barsoum [3] studied the stability analysis of structural systems under non-conservative forces using Hamilton principle as basis and the dynamic criterion of stability. Attard and Somervaille [4] focused on free vibration analysis of straight prismatic beams of general thin-walled open cross-section, under conservative and nonconservative loads. Joshi and Suryanarayan [5] investigated coupled flexural-torsional vibrations of double-symmetric thin-wall beams under axial loads and end moments. They found that the problem could be reduced to a beam-column problem with a zero moment, so that it was possible to obtain simple algebraic expressions unifying numerical results for various boundary conditions. Based on the transfer matrix method, Ohga et al. [6, 7] estimated not only the natural frequencies but also vibration mode shapes of the thin-walled members under in-plane forces. Mohri et al. [8] presented a higher-order non shear deformable model to investigate the dynamic behavior of thin-walled open sections in the pre- and post-buckling state. In their numeric examples, they considered simply supported beams under axial and distributed transverse loads. Silvestre and Camotim [9] derived of a Generalised Beam Theory (GBT) to analyse the vibration behaviour of loaded cold-formed steel members. Later, they [10] continued to study local and global vibration of thin-walled members under compression and non-uniform bending. The geometrically nonlinear stiffness reduction caused by the presence of longitudinal stress gradients and the ensuing shear stresses was taken into account in the formulation. Voros [11] analyzed the free vibration and mode shapes of straight beams where the coupling between the bending and torsion was induced by steady state lateral loads. Closed form solution for the coupled frequencies and mode shapes of a symmetric beam with simply supported ends under uniform bending was derived. By using the power series method, Leung [12,13] developed the exact dynamic stiffness matrix including both the axial force, initial torque and bending moment for the interactive axial-torsional and axial-moment buckling analysis of framed structures. Recently, Leung [14] proposed a new concept of uniform torque for buckling of columns by biaxial moments and uniform end torque. Second-order effects of the axial force, biaxial moments and torque were considered in the analysis.

For thin-walled composite beams, due to coupling effects from material anisotropy, these members under combined axial force and bending loads simultaneously exhibit strong coupling. Therefore, their dynamic characteristics and load-frequency interaction curves become very complicated. Several authors have investigated the free vibration

characters of axially loaded composite beams (Banerjee et al. [15,16], Li et al. [17,18] , Kaya and Ozgumus [19] and Emam and Nayfeh [20]) but only a few have taken into account the effects of axial force and bending loads. By extending GBT formulation, Silvestre and Camotim [21] investigated the local and global vibration behavior of loaded thin-walled composite members, focusing on issues dealing with the variation of the fundamental frequency and vibration mode nature with the member length and applied stress level. Machado and Cortinez [22] presented free vibration of thin-walled composite beams with static initial stresses and deformations. The analysis was based on a geometrically non-linear theory based on large displacements and rotations. However, it was strictly valid for symmetric balanced laminates and especially orthotropic laminates. It is clear that the research of the vibration of thin-walled composite beams with arbitrary lay-ups under combined axial force and bending loads in a unitary manner is limited. This complicated problem has received scant attention and there is a need for further studies.

In this paper, which is an extension of the authors' previous works [23-26], vibration analysis of thin-walled composite beams with arbitrary lay-ups under combined axial force and bending loads is presented. This model is based on the classical lamination theory, and accounts for all the structural coupling coming from the material anisotropy. The governing differential equations for flexural-torsional coupled vibration are derived from the Hamilton's principle. A displacement-based one-dimensional finite element model is developed to solve the problem. Numerical results are obtained for thin-walled composite beams to investigate the effects of axial force, bending loads, fiber orientation on the natural frequencies and load-frequency interaction curves as well as vibration mode shapes.

2. KINEMATICS

The theoretical developments presented in this paper require two sets of coordinate systems which are mutually interrelated. The first coordinate system is the orthogonal Cartesian coordinate system (x, y, z), for which the x and y axes lie in the plane of the cross section and the z axis parallel to the longitudinal axis of the beam. The second coordinate system is the local plate coordinate (n, s, z) as shown in Fig. 1, wherein the n axis is normal to the middle surface of a plate element, the s axis is tangent to the middle surface and is directed along the contour line of the cross section. The (n, s, z) and (x, y, z) coordinate systems are related through an angle of orientation α. As defined in Fig.1 a point P, called the pole, is placed at an arbitrary point x_p, y_p. A line through P parallel to the z axis is called the pole axis.

To derive the analytical model for a thin-walled composite beam, the following assumptions are made

1. The contour of the thin wall does not deform in its own plane.

2. The linear shear strain $\bar{\gamma}_{sz}$ of the middle surface is zero in each element.

3. The Kirchhoff-Love assumption in classical plate theory remains valid for laminated composite thin-walled beams.

4. Each laminate is thin and perfectly bonded.

According to assumption 1, the midsurface displacement components $\bar{u}, \bar{v}$ at a point A in the contour coordinate system can be expressed in terms of a displacements U, V of the pole P in the x, y directions, respectively, and the rotation angle Φ about the pole axis,

$$\bar{u}(s, z) = U(z)\sin\alpha(s) - V(z)\cos\alpha(s) - \Phi(z)q(s) \tag{1a}$$

$$\bar{v}(s, z) = U(z)\cos\alpha(s) + V(z)\sin\alpha(s) + \Phi(z)r(s) \tag{1b}$$

These equations apply to the whole contour. The out-of-plane shell displacement $\bar{w}$ can now be found from the assumption 2. For each element of middle surface, the shear strain become

$$\bar{\gamma}_{sz} = \frac{\partial\bar{v}}{\partial z} + \frac{\partial\bar{w}}{\partial s} = 0 \tag{2}$$

Eq.(2) can be integrated with respect to s from the origin to an arbitrary point on the contour,

$$\bar{w}(s, z) = W(z) - U'(z)x(s) - V'(z)y(s) - \Phi'(z)\omega(s) \tag{3}$$

where differentiation with respect to the axial coordinate z is denoted by primes $(')$; W represents the average axial displacement of the beam in the z direction; x and y are the coordinates of the contour in the (x, y, z) coordinate system; and ω is the so-called sectorial coordinate or warping function given by

$$\omega(s) = \int_{s_\circ}^{s} r(s)ds \tag{4a}$$

The displacement components u, v, w representing the deformation of any generic point on the profile section are given with respect to the midsurface displacements $\bar{u}, \bar{v}, \bar{w}$ by the assumption 3.

$$u(s, z, n) = \bar{u}(s, z) \tag{5a}$$

$$v(s, z, n) = \bar{v}(s, z) - n\frac{\partial\bar{u}(s, z)}{\partial s} \tag{5b}$$

$$w(s, z, n) = \bar{w}(s, z) - n\frac{\partial\bar{u}(s, z)}{\partial z} \tag{5c}$$

The strains associated with the small-displacement theory of elasticity are given by

$$\epsilon_z = \bar{\epsilon}_z + n\bar{\kappa}_z \tag{6a}$$

$$\gamma_{sz} = n\bar{\kappa}_{sz} \tag{6b}$$

where

$$\bar{\epsilon}_z = \frac{\partial \bar{w}}{\partial z} \tag{7a}$$

$$\bar{\kappa}_z = -\frac{\partial^2 \bar{u}}{\partial z^2} \tag{7b}$$

$$\bar{\kappa}_{sz} = -2\frac{\partial^2 \bar{u}}{\partial s \partial z} \tag{7c}$$

All the other strains are identically zero. In Eq.(7), $\bar{\epsilon}_z$, $\bar{\kappa}_z$ and $\bar{\kappa}_{sz}$ are midsurface axial strain and biaxial curvature of the shell, respectively. The above shell strains can be converted to beam strain components by substituting Eqs.(1), (3) and (5) into Eq.(7) as

$$\bar{\epsilon}_z = \epsilon_z^\circ + x\kappa_y + y\kappa_x + \omega\kappa_\omega \tag{8a}$$

$$\bar{\kappa}_z = \kappa_y \sin\alpha - \kappa_x \cos\alpha - \kappa_\omega q \tag{8b}$$

$$\bar{\kappa}_{sz} = \kappa_{sz} \tag{8c}$$

where $\epsilon_z^\circ, \kappa_x, \kappa_y, \kappa_\omega$ and κ_{sz} are axial strain, biaxial curvatures in the x and y direction, warping curvature with respect to the shear center, and twisting curvature in the beam, respectively defined as

$$\epsilon_z^\circ = W' \tag{9a}$$

$$\kappa_x = -V'' \tag{9b}$$

$$\kappa_y = -U'' \tag{9c}$$

$$\kappa_\omega = -\Phi'' \tag{9d}$$

$$\kappa_{sz} = 2\Phi' \tag{9e}$$

The resulting strains can be obtained from Eqs.(6) and (8) as

$$\epsilon_z = \epsilon_z^\circ + (x + n\sin\alpha)\kappa_y + (y - n\cos\alpha)\kappa_x + (\omega - nq)\kappa_\omega \tag{10a}$$

$$\gamma_{sz} = n\kappa_{sz} \tag{10b}$$

3. VARIATIONAL FORMULATION

The total potential energy of the system can be stated, in its buckled shape, as

$$\Pi = \mathcal{U} + \mathcal{V} \tag{11}$$

where $\mathcal{U}$ is the strain energy

$$\mathcal{U} \;=\; \frac{1}{2}\int_v (\sigma_z\epsilon_z + \sigma_{sz}\gamma_{sz})dv \tag{12}$$

After substituting Eq.(10) into Eq.(12), the variation of strain energy can be stated as

$$\delta\mathcal{U} \;=\; \int_0^l (N_z\delta\epsilon_z + M_y\delta\kappa_y + M_x\delta\kappa_x + M_\omega\delta\kappa_\omega + M_t\delta\kappa_{sz})dz \tag{13}$$

where $N_z, M_x, M_y, M_\omega, M_t$ are axial force, bending moments in the x- and y-direction, warping moment (bimoment), and torsional moment with respect to the centroid, respectively, defined by integrating over the cross-sectional area A as

$$N_z \;=\; \int_A \sigma_z ds dn \tag{14a}$$

$$M_y \;=\; \int_A \sigma_z(x + n\sin\alpha)ds dn \tag{14b}$$

$$M_x \;=\; \int_A \sigma_z(y - n\cos\alpha)ds dn \tag{14c}$$

$$M_\omega \;=\; \int_A \sigma_z(\omega - nq)ds dn \tag{14d}$$

$$M_t \;=\; \int_A \sigma_{sz} n ds dn \tag{14e}$$

The variation of the potential of the in-plane load N_0 at the centroid and transverse load p acting on the cross section at a point a distance $\bar{a}$ above the shear center can be found in Refs. [23, 24]

$$\delta\mathcal{V} \;=\; \int_0^l \Big[N_0\big[\delta U'(U' + \Phi'y_p) + \delta V'(V' - \Phi'x_p) + \delta\Phi'(\Phi'\frac{I_p}{A} + U'y_p - V'x_p)\big]$$
$$-\; M_b(\Phi\delta U'' + U''\delta\Phi) - \bar{a}p\Phi\delta\Phi\Big]dz \tag{15}$$

where M_b is not the actual bending moment in the beam, but the simple beam moment due to transverse load p.

The variation of the kinetic energy is expressed in Ref. [25] as

$$\delta\mathcal{T} \;=\; \int_0^l \Big[m_0\dot{W}\delta\dot{W} + \big[m_0\dot{U} + (m_c + m_0 y_p)\dot{\Phi}\big]\delta\dot{U} + \big[m_0\dot{V} + (m_s - m_0 x_p)\dot{\Phi}\big]\delta\dot{V}$$
$$+\; \big[(m_c + m_0 y_p)\dot{U} + (m_s - m_0 x_p)\dot{V} + (m_p + m_2 + 2m_\omega)\dot{\Phi}\big]\delta\dot{\Phi}\Big]dz \tag{16}$$

where, m_0, m_c, m_p, m_s, m_2 are inertia coefficients. In order to derive the equations of motion, Hamilton's principle is used

$$\delta\int_{t_1}^{t_2} (\mathcal{T} - \Pi)dt \;=\; 0 \tag{17}$$

107 Substituting Eqs.(13),(15) and (16) into Eq.(17), the following weak statement is obtained

$$
\begin{aligned}
0 = \int_{t_1}^{t_2} \int_0^l & \Big\{ m_0 \dot{W} \delta \dot{W} + \big[m_0 \dot{U} + (m_c + m_0 y_p) \dot{\Phi} \big] \delta \dot{U} + \big[m_0 \dot{V} + (m_s - m_0 x_p) \dot{\Phi} \big] \delta \dot{V} \\
& + \big[(m_c + m_0 y_p) \dot{U} + (m_s - m_0 x_p) \dot{V} + (m_p + m_2 + 2 m_\omega) \dot{\Phi} \big] \delta \dot{\Phi} \\
& - \Big[N_0 \big[\delta U'(U' + \Phi' y_p) + \delta V'(V' - \Phi' x_p) + \delta \Phi'(\Phi' \frac{I_p}{A} + U' y_p - V' x_p) \big] - M_b (\Phi \delta U'' + U'' \delta \Phi) - \bar{a} p \Phi \delta \Phi \Big] \\
& - N_z \delta W' + M_y \delta U'' + M_x \delta V'' + M_\omega \delta \Phi'' - 2 M_t \delta \Phi \Big\} dz dt
\end{aligned} \tag{18}
$$

108 In Eq.(18), M_b and p are the buckling moment and transverse load, and can be written for various types of loading

109 as

$$
M_b = \lambda f(z) \tag{19a}
$$

$$
p = \lambda g(z) \tag{19b}
$$

110 where λ is a buckling parameter and $f(z)$ and $g(z)$ are polynomial functions which depend on the loading pattern.

111 These functions are given as follows for various types of loading:

$$
\begin{cases}
f(z) = 1; \quad g(z) = 0 & \text{for pure bending} \\
f(z) = \frac{1}{2}(\frac{l^2}{4} - z^2); \quad g(z) = 1 & \text{for uniformly distributed load} \\
f(z) = \frac{l}{2} - z; \quad g(z) = \begin{cases} 0 \\ 1 \text{ at the loading point} \end{cases} & \text{for point load at free end of a cantilever beam}
\end{cases} \tag{20}
$$

4. CONSTITUTIVE EQUATIONS

113 The constitutive equations of a kth orthotropic lamina in the laminate co-ordinate system of section are given by

$$
\left\{ \begin{array}{c} \sigma_z \\ \sigma_{sz} \end{array} \right\}^k = \left[\begin{array}{cc} \bar{Q}_{11}^* & \bar{Q}_{16}^* \\ \bar{Q}_{16}^* & \bar{Q}_{66}^* \end{array} \right]^k \left\{ \begin{array}{c} \epsilon_z \\ \gamma_{sz} \end{array} \right\} \tag{21}
$$

114 where $\bar{Q}_{ij}^*$ are transformed reduced stiffnesses. The transformed reduced stiffnesses can be calculated from the

115 transformed stiffnesses based on the plane stress ($\sigma_s = 0$) and plane strain ($\epsilon_s = 0$) assumption. More detailed

116 explanation can be found in Ref. [27].

117   The constitutive equations for bar forces and bar strains are obtained by using Eqs.(10), (14) and (21)

$$
\begin{Bmatrix} N_z \\ M_y \\ M_x \\ M_\omega \\ M_t \end{Bmatrix} = \begin{bmatrix} E_{11} & E_{12} & E_{13} & E_{14} & E_{15} \\ & E_{22} & E_{23} & E_{24} & E_{25} \\ & & E_{33} & E_{34} & E_{35} \\ & & & E_{44} & E_{45} \\ \text{sym.} & & & & E_{55} \end{bmatrix} \begin{Bmatrix} \epsilon_z^\circ \\ \kappa_y \\ \kappa_x \\ \kappa_\omega \\ \kappa_{sz} \end{Bmatrix} \tag{22}
$$

118   where E_{ij} are stiffnesses of thin-walled composite beams and given in Ref. [25].

5. GOVERNING EQUATIONS OF MOTION

120   The governing equations of motion of the present study can be derived by integrating the derivatives of the varied

121   quantities by parts and collecting the coefficients of of $\delta W, \delta U, \delta V$ and $\delta \Phi$

$$N_z' = m_0 \ddot{W} \tag{23a}$$

$$M_y'' + N_0\big(U'' + \Phi'' y_p\big) + (M_b \Phi)'' = m_0 \ddot{U} + (m_c + m_0 y_p)\ddot{\Phi} \tag{23b}$$

$$M_x'' + N_0\big(V'' - \Phi'' x_p\big) = m_0 \ddot{V} + (m_s - m_0 x_p)\ddot{\Phi} \tag{23c}$$

$$M_\omega'' + 2M_t' + N_0\big(\Phi'' \frac{I_p}{A} + U'' y_p - V'' x_p\big) + M_b U'' + \bar{a} p \Phi = (m_c + m_0 y_p)\ddot{U}$$

$$+ \ (m_s - m_0 x_p)\ddot{V}$$

$$+ \ (m_p + m_2 + 2m_\omega)\ddot{\Phi} \tag{23d}$$

122   By substituting Eqs.(9) and (22) into Eq.(23), the explicit form of governing equations of motion can be expressed

with respect to the laminate stiffnesses E_{ij} as

$$E_{11}W'' - E_{12}U''' - E_{13}V''' - E_{14}\Phi''' + 2E_{15}\Phi'' = m_0\ddot{W} \tag{24a}$$

$$E_{12}W''' - E_{22}U^{iv} - E_{23}V^{iv} - E_{24}\Phi^{iv} + 2E_{25}\Phi'''$$
$$+N_0(U'' + \Phi''y_p) + (M_b\Phi)'' = m_0\ddot{U} + (m_c + m_0y_p)\ddot{\Phi} \tag{24b}$$

$$E_{13}W''' - E_{23}U^{iv} - E_{33}V^{iv} - E_{34}\Phi^{iv} + 2E_{35}\Phi'''$$
$$+N_0(V'' - \Phi''x_p) = m_0\ddot{V} + (m_s - m_0x_p)\ddot{\Phi} \tag{24c}$$

$$E_{14}W''' + 2E_{15}W'' - E_{24}U^{iv} - 2E_{25}U''' - E_{34}V^{iv} - 2E_{35}V'''$$
$$-E_{44}\Phi^{iv} + 4E_{55}\Phi'' + N_0(\Phi''\frac{I_p}{A} + U''y_p - V''x_p) + M_bU'' + \bar{a}p\Phi = (m_c + m_0y_p)\ddot{U}$$
$$+ (m_s - m_0x_p)\ddot{V}$$
$$+ (m_p + m_2 + 2m_\omega)\ddot{\Phi} \tag{24d}$$

Eq.(24) is most general form for flexural-torsional coupled vibration of thin-walled composite beams with arbitrary lay-ups under axial and bending loads and the dependent variables, W, U, V and Φ are fully coupled. For the case of thin-walled composite beams under axial force and uniform bending, if all the coupling effects and the cross section is symmetrical with respect to both x- and the y-axes, Eq.(24) can be simplified to the uncoupled differential equations as

$$(EA)_{com}W'' = \rho A\ddot{W} \tag{25a}$$

$$-(EI_y)_{com}U^{iv} + N_0U'' + M_b\Phi'' = \rho A\ddot{U} \tag{25b}$$

$$-(EI_x)_{com}V^{iv} + N_0V'' = \rho A\ddot{V} \tag{25c}$$

$$-(EI_\omega)_{com}\Phi^{iv} + \left[(GJ)_{com} + N_0\frac{I_p}{A}\right]\Phi'' + M_bU'' = \rho I_p\ddot{\Phi} \tag{25d}$$

From above equations, $(EA)_{com}$ represents axial rigidity, $(EI_x)_{com}$ and $(EI_y)_{com}$ represent flexural rigidities with respect to x- and y-axis, $(EI_\omega)_{com}$ represents warping rigidity, and $(GJ)_{com}$ represents torsional rigidity of thin-

walled composite beams, respectively, written as

$$(EA)_{com} = E_{11} \tag{26a}$$

$$(EI_y)_{com} = E_{22} \tag{26b}$$

$$(EI_x)_{com} = E_{33} \tag{26c}$$

$$(EI_\omega)_{com} = E_{44} \tag{26d}$$

$$(GJ)_{com} = 4E_{55} \tag{26e}$$

6. ANALYTICAL SOLUTIONS FOR SIMPLY SUPPORTED COMPOSITE BEAMS UNDER AXIAL FORCE AND UNIFORM BENDING

For simply supported beams with free warping, the overall displacements modes in bending and torsion are assumed as

$$U(z,t) = U_0 \sin(\frac{n\pi z}{L}) \sin(\omega t) \tag{27a}$$

$$V(z,t) = V_0 \sin(\frac{n\pi z}{L}) \sin(\omega t) \tag{27b}$$

$$\Phi(z,t) = \Phi_0 \sin(\frac{n\pi z}{L}) \sin(\omega t) \tag{27c}$$

Substituting Eq.(27) into Eq.(25), after integrations and some reductions, the resulting flexural and torsional equations of motion are obtained in compact form as

$$\omega_{x_n}^2(1 - \overline{P}_{x_n}) - \omega_{xx_n}^2 = 0 \tag{28a}$$

$$A\Big[\omega_{y_n}^2(1 - \overline{P}_{y_n}) - \omega^2\Big]U_0 - \overline{M}_{x_n}\sqrt{AI_p}\omega_{y_n}\omega_{\theta_n}\Phi_0 = 0 \tag{28b}$$

$$-\overline{M}_{x_n}\sqrt{AI_p}\omega_{y_n}\omega_{\theta_n}U_0 + I_p\Big[\omega_{\theta_n}^2(1 - \overline{P}_{\theta_n}) - \omega^2\Big]\Phi_0 = 0 \tag{28c}$$

For the above equations, it is well known that the flexural natural frequencies in the x-direction and bending moments are decoupled, while, the flexural natural frequencies in the y-direction, torsional natural frequencies and bending moments are coupled. They are given by the orthotropy solution for simply supported boundary condition

$$\omega_{xx_n} = \omega_{x_n}\sqrt{1 - \overline{P}_{x_n}} \tag{29a}$$

$$\omega_{ya_n} = \sqrt{\frac{\omega_{y_n}^2(1 - \overline{P}_{y_n}) + \omega_{\theta_n}^2(1 - \overline{P}_{\theta_n})}{2} - \sqrt{\Big[\frac{\omega_{y_n}^2(1 - \overline{P}_{y_n}) - \omega_{\theta_n}^2(1 - \overline{P}_{\theta_n})}{2}\Big]^2 + \overline{M}_{x_n}^2\omega_{y_n}^2\omega_{\theta_n}^2}} \tag{29b}$$

$$\omega_{yb_n} = \sqrt{\frac{\omega_{y_n}^2(1 - \overline{P}_{y_n}) + \omega_{\theta_n}^2(1 - \overline{P}_{\theta_n})}{2} + \sqrt{\Big[\frac{\omega_{y_n}^2(1 - \overline{P}_{y_n}) - \omega_{\theta_n}^2(1 - \overline{P}_{\theta_n})}{2}\Big]^2 + \overline{M}_{x_n}^2\omega_{y_n}^2\omega_{\theta_n}^2}} \tag{29c}$$

in which $\omega_{x_n}, \omega_{y_n}$ and ω_{θ_n} are the flexural natural frequencies in the x- and y-direction, and torsional natural frequencies [28]

$$\omega_{x_n} = \frac{n^2\pi^2}{l^2}\sqrt{\frac{(EI_x)_{com}}{\rho A}} \tag{30a}$$

$$\omega_{y_n} = \frac{n^2\pi^2}{l^2}\sqrt{\frac{(EI_y)_{com}}{\rho A}} \tag{30b}$$

$$\omega_{\theta_n} = \frac{n\pi}{l}\sqrt{\frac{1}{\rho I_p}\Big[\frac{n^2\pi^2}{l^2}(EI_\omega)_{com} + (GJ)_{com}\Big]} \tag{30c}$$

and $\overline{P}_{x_n}, \overline{P}_{y_n}, \overline{P}_{\theta_n}$ and $\overline{M}_{x_n}$ are nondimensional axial force and moment.

$$\overline{P}_{x_n} = \frac{N_0}{P_{x_n}} \tag{31a}$$

$$\overline{P}_{y_n} = \frac{N_0}{P_{y_n}} \tag{31b}$$

$$\overline{P}_{\theta_n} = \frac{N_0}{P_{\theta_n}} \tag{31c}$$

$$\overline{M}_{x_n} = \frac{M_b}{M_{cr_n}} \tag{31d}$$

where P_{x_n}, P_{y_n} and P_{θ_n} are the flexural buckling loads in the x- and y-direction, and torsional buckling loads [29]

$$P_{x_n} = \frac{n^2\pi^2(EI_x)_{com}}{l^2} \tag{32a}$$

$$P_{y_n} = \frac{n^2\pi^2(EI_y)_{com}}{l^2} \tag{32b}$$

$$P_{\theta_n} = \frac{A}{I_p}\Big[\frac{n^2\pi^2(EI_\omega)_{com}}{l^2} + (GJ)_{com}\Big] \tag{32c}$$

and M_{cr_n} is the buckling moments for pure bending [29]

$$M_{cr_n} = \sqrt{\frac{n^2\pi^2(EI_y)_{com}}{l^2}\Big[\frac{n^2\pi^2(EI_\omega)_{com}}{l^2} + (GJ)_{com}\Big]} \tag{33}$$

7. FINITE ELEMENT FORMULATION

The present theory for thin-walled composite beams described in the previous section was implemented via a displacement based finite element method. The element has seven degrees of freedom at each node, three displacements W, U, V and three rotations U', V', Φ as well as one warping degree of freedom Φ'. The axial displacement W is interpolated using linear shape functions Ψ_j, whereas the lateral and vertical displacements U, V and axial rotation Φ

are interpolated using Hermite-cubic shape functions ψ_j associated with node j and the nodal values, respectively.

$$W = \sum_{j=1}^{2} w_j \Psi_j \tag{34a}$$

$$U = \sum_{j=1}^{4} u_j \psi_j \tag{34b}$$

$$V = \sum_{j=1}^{4} v_j \psi_j \tag{34c}$$

$$\Phi = \sum_{j=1}^{4} \phi_j \psi_j \tag{34d}$$

Substituting these expressions into the weak statement in Eq.(18), the finite element model of a typical element can be expressed as the standard eigenvalue problem

$$([K] - N_0[G_1] - \lambda[G_2] - \omega^2[M])\{\Delta\} = \{0\} \tag{35}$$

where $[K], [G_1], [G_2]$ and $[M]$ are the element stiffness matrix, the element geometric stiffness matrix due to axial force and bending loads as well as the element mass matrix, respectively. The explicit forms of them are given in Refs. [23-26].

In Eq.(35), $\{\Delta\}$ is the eigenvector of nodal displacements corresponding to an eigenvalue

$$\{\Delta\} = \{W \ U \ V \ \Phi\}^{\mathrm{T}} \tag{36}$$

8. NUMERICAL EXAMPLES

A thin-walled composite I-beam with length $l = 8\text{m}$ is considered to investigate the effects of axial force, bending loads, fiber orientation on the natural frequencies and load-frequency interaction curves as well as vibration mode shapes. The geometry of the I-section is shown in Fig. 2. Stacking sequence of this beam consists of two layers with equal thickness as follows: angle-ply laminate $[\theta/-\theta]$ at the bottom flange, and unidirectional laminate $[0]_2$ at the top flange and web, respectively. For this lay-up, all the coupling stiffnesses are zero, but E_{15} and E_{35} do not vanish. The following engineering constants are used

$$E_1/E_2 = 25, G_{12}/E_2 = 0.6, \nu_{12} = 0.25 \tag{37}$$

For convenience, the following nondimensional axial force, bending loads and natural frequency are used

$$\overline{N}_{cr} = \frac{N_{cr}l^2}{E_2 t b_3^3} \tag{38a}$$

$$\overline{M}_{cr} = \frac{M_{cr}l}{E_2 t b_3^3} \tag{38b}$$

$$\overline{P}_{cr} = \frac{P_{cr}l^2}{E_2 t b_3^3} \tag{38c}$$

$$\overline{q}_{cr} = \frac{q_{cr}l^3}{E_2 t b_3^3} \tag{38d}$$

$$\overline{\omega} = \frac{\omega l^2}{b_3}\sqrt{\frac{\rho}{E_2}} \tag{38e}$$

As a first example, a simply-supported composite beam under under uniformly distributed load is analyzed. The load is applied at at the shear center, top flange and bottom flange. The first load-frequency interaction curves for three cases are plotted with respect to the fiber angle variation in Fig. 3. It is clear that the location of applied load has major effects of vibration of beams under transverse load. All three cases of groups show similar trends. That is, the smallest group is for the case of load at the top flange and the largest one is for the case of load at the bottom flange. The lowest three load-frequency interaction curves with fiber angles $\theta = 0°$, $30°$ and $60°$ for three cases are displayed in Figs. 4, 5 and 6. At $\theta = 0°$ (Fig. 4), the first and third natural frequencies decrease from $\overline{\omega}_1 = 5.05$ and $\overline{\omega}_3 = 20.15$ to zero, when the lateral buckling loads are reached, depending on the position of the load height, vice versa, the second one increases monotonically with the increase of load. As the fiber angle changes, this response is no longer visible. For example, at $\theta = 30°$, for the case of load at shear center, with the increase of load, the first and third natural frequencies increase and reach local maximum values around $\overline{q} = 0.39$ and 0.51, they decrease and finally vanish at $\overline{q}_{cr_1} = 0.45$ and $\overline{q}_{cr_2} = 1.64$, respectively, which are corresponding to the first and second lateral buckling loads (Fig. 5). The decrease becomes more quickly when uniform loads are close to lateral buckling loads.

The next example is a simply supported composite beam under combined axial force and bending moment. The lowest four natural frequencies are obtained by the finite element analysis and orthotropy solution, which neglects the coupling effects of E_{15} and E_{35} from Eqs.(29a)-(29c), are given in Table 1. The critical flexural-torsional buckling loads ($\overline{N}_{cr}$) and critical buckling moments ($\overline{M}_{cr}$) for pure bending agree completely with those of previous papers [23,24]. With the same value of bending moment, it can be seen that the natural frequencies diminish when the axial force changes from tensile to compressive, as expected. For unidirectional fiber direction, the lowest four natural frequencies by the finite element analysis exactly corresponding to the flexural-torsional coupled modes and the first flexural mode in x-direction by the orthotropy solution, respectively. As the fiber angle is rotated off-axis, the orthotropy solution and finite element analysis solution show discrepancy indicating the coupling effects become significant. It can be

also explained partly by the typical normal mode shapes corresponding to the first four natural frequencies with fiber angle $\theta = 30°$ for the case $(\overline{N} = 0.5\overline{N}_{cr}, \overline{M} = 0.5\overline{M}_{cr})$ in Fig. 7. It should be noticed that although a coupling stiffness E_{15} between the axial mode and the torsional mode is not null, the magnitude of induced axial displacement W is much lower than U, V and Φ and thus, is not plotted in the mode shapes. As a result, the first three natural frequency exhibits doubly coupled modes (flexural mode in y-direction and torsional mode), whereas, the fourth one displays triply coupled modes (flexural mode in the x-, y-direction and torsional mode). Therefore, the orthotropy solution is no longer valid for unsymmetrically laminated beams due to coupling effects. In order to investigate these effects further in the large bending moment region, the lowest three moment-frequency interaction curves with the fiber angle $\theta = 30°$ for two cases $(\overline{N} = 0)$ and $(\overline{N} = 0.5\overline{N}_{cr})$ are displayed in Figs. 8 and 9. These figures highlight the effects of coupling on the vibration of thin-walled composite beam under axial load and bending moment. It is very interesting to note that all moment-frequency interaction curves by finite element analysis are asymmetric. This response is never seen in isotropic beams with doubly symmetric cross-section because coupling terms are not present. For the case $(\overline{N} = 0.5\overline{N}_{cr})$ in Fig. 9, due to asymmetric interaction curves, when the natural frequency vanishes, each branch always has two different buckling moments. For instance, at the lowest branch, the negative buckling moment, $\overline{M}_{cr_1} = -2.50 \times 10^{-2}$, occurs when the moment causes tension in the top flange, while the positive one, $\overline{M}_{cr_2} = 3.72 \times 10^{-2}$, corresponds to a reversal in the sense of the moment which causes compression in the top flange. As a result, this branch is disappeared when $\overline{M}$ is slightly outside this range. As the bending moment changes, two interaction curves $(\omega_2 - M_2)$ and $(\omega_3 - M_3)$ intersect at $\overline{M} = -7.20 \times 10^{-2}$ and $\overline{M} = 12.20 \times 10^{-2}$, thus, after these values, vibration mode 2 and 3 change each other. The second branch will also be disappeared when $\overline{M}$ is slightly outside the range of $[-12.88 \quad 14.10] \times 10^{-2}$.

The last example is the same as before except that in this case, boundary condition is clamped-free. A cantilever composite beam under combined axial force and vertical point load at shear center of free end is considered. Effect of axial force on the first load-frequency interaction curves of fiber angles $30°$ and $60°$ is investigated. Three cases of axial force is considered in Fig. 10. Both lateral buckling loads and natural frequencies increase when the axial force changes from compressive to tensile. It demonstrated again the fact that tensile forces stiffen the beam while compressive forces soften the beam. Three dimensional interaction diagram of the fundamental natural frequency, vertical load with respect to the axial compressive force change of these angles is plotted in Fig. 11. As expected, load-frequency interaction curves become smaller as the axial force increases and finally vanish at about $\overline{N} = 0.79$ and 0.57 for $\theta = 30°$ and $60°$, respectively, which implies that at these loads, the critical flexural-torsional buckling occur as

a degenerated case of natural vibration and vertical load at zero value. It is from this figure that illustrate clearly the characteristic of load-load-frequency interaction curve, which explains the duality between flexural-torsional buckling load, lateral buckling load and natural frequency.

9. CONCLUDING REMARKS

A one-dimensional finite element model was developed to study the vibration analysis of thin-walled composite beams with I-section. This model has been applied to the investigation of load-frequency interaction curves of beams under uniformly distributed load, combined axial force and bending loads. The effects of loading condition, location of applied load and fiber orientation on the natural frequencies, load-frequency interaction curves and mode shapes are investigated. Triply coupled vibration modes including the flexural mode in the x-, y-direction and torsional mode are included in the analysis. The present model is found to be appropriate and efficient in analyzing vibration problem of thin-walled composite beams under combined axial force and bending loads.

References

[1] V. Z. Vlasov, Thin Walled Elastic Beams, Israel Program for Scientific Transactions, Jerusalem, 1961.

[2] A. Gjelsvik, The theory of thin walled bars, Wiley, New York, 1981.

[3] R. S. Barsoum, Finite element method applied to the problem of stability of a non-conservative system, Int J Numer Meth Eng 3 (1) (1971) 63–87.

[4] M. M. Attard, I. J. Somervaille, Stability of thin-walled open beams under nonconservative loads, Mech Struct Mach 15 (3) (1987) 395 – 412.

[5] A. Joshi, S. Suryanarayan, Unified analytical solution for various boundary conditions for the coupled flexural-torsional vibration of beams subjected to axial loads and end moments, J Sound Vib 129 (2) (1989) 313 – 326.

[6] M. Ohga, K. Nishimato, T. Shigematsu, T. Hara, Natural frequencies and mode shapes of thin-walled members under in-plane forces., in: Thin-Walled Structures Research and Development, Second International Conference on Thin-Walled Structures, Elsevier, 1998:501–508.

[7] M. Ohga, T. Shigematsu, T. Hara, Natural frequencies and mode shapes of thin-walled members with shell type cross section, Steel Compos Struct 2 (3) (2002) 223–236.

[8] F. Mohri, L. Azrar, M. Potier-Ferry, Vibration analysis of buckled thin-walled beams with open sections, J Sound Vib 275 (1-2) (2004) 434 – 446.

[9] N. Silvestre, D. Camotim, Vibration behaviour of axially compressed cold-formed steel members, Steel Compos Struct 6 (3) (2006) 221–236.

[10] R. Bebiano, N. Silvestre, D. Camotim, Local and global vibration of thin-walled members subjected to compression and non-uniform bending, J Sound Vib 315 (3) (2008) 509 – 535.

[11] G. M. Voros, On coupled bending-torsional vibrations of beams with initial loads, Mech Res Commun 36 (5) (2009) 603 – 611.

[12] A. Y. T. Leung, Exact dynamic stiffness for axial-torsional buckling of structural frames, Thin-Walled Struct 46 (1) (2008) 1 – 10.

[13] A. Y. T. Leung, Dynamic axial-moment buckling of linear beam systems by power series stiffness, J Eng Mech 135 (8) (2009) 852–861.

[14] A. Y. T. Leung, Dynamic buckling of columns by biaxial moments and uniform end torque, J Sound Vib 329 (11) (2010) 2218 – 2240.

[15] J. R. Banerjee, F. W. Williams, Exact dynamic stiffness matrix for composite Timoshenko beams with applications, J Sound Vib 194 (4) (1996) 573 – 585.

[16] J. R. Banerjee, Free vibration of axially loaded composite Timoshenko beams using the dynamic stiffness matrix method, Comput Struct 69 (2) (1998) 197 – 208.

[17] J. Li, R. Shen, H. Hua, J. Xianding, Bending-torsional coupled dynamic response of axially loaded composite Timosenko thin-walled beam with closed cross-section, Compos Struct 64 (1) (2004) 23 – 35.

[18] J. Li, H. Hua, R. Shen, Dynamic stiffness analysis for free vibrations of axially loaded laminated composite beams, Compos Struct 84 (1) (2008) 87 – 98.

[19] M. Kaya, O. O. Ozgumus, Flexural-torsional-coupled vibration analysis of axially loaded closed-section composite Timoshenko beam by using DTM, J Sound Vib 306 (3-5) (2007) 495 – 506.

[20] S. A. Emam, A. H. Nayfeh, Postbuckling and free vibrations of composite beams, Compos Struct 88 (4) (2009) 636 – 642.

[21] N. Silvestre, D. Camotim, Gbt-based local and global vibration analysis of loaded composite open-section thin-walled members, Int J Struct Stab Dy 6 (1) (2006) 1–29.

[22] S. P. Machado, V. H. Cortinez, Free vibration of thin-walled composite beams with static initial stresses and deformations, Eng Struct 29 (3) (2007) 372 – 382.

[23] J. Lee, S. E. Kim, Flexural-torsional buckling of thin-walled I-section composites, Comput Struct 79 (10) (2001) 987 – 995.

[24] J. Lee, S. E. Kim, K. Hong, Lateral buckling of I-section composite beams, Eng Struct 24 (7) (2002) 955 – 964.

[25] J. Lee, S. E. Kim, Free vibration of thin-walled composite beams with I-shaped cross-sections, Compos Struct 55 (2) (2002) 205 – 215.

[26] J. Lee, S. Lee, Flexural-torsional behavior of thin-walled composite beams, Thin-Walled Struct 42 (9) (2004) 1293 – 1305.

[27] R. M. Jones, Mechanics of Composite Materials, Taylor & Francis, 1999.

[28] S. Timoshenko, D. H. Young, W. J. R. Weaver, Vibration problems in engineering, John Wiley & Sons, New York, 1974.

[29] S. Timoshenko, J. M. Gere, Theory of elastic stability, McGraw-Hill, New York, 1961.

CAPTIONS OF TABLES

Table 1: Effect of axial force and bending moment on the first four natural frequencies with respect to the fiber angle change in the bottom flange of a simply supported composite beam.

CAPTIONS OF FIGURES

Figure 1: Definition of coordinates in thin-walled open sections.

Figure 2: Geometry of thin-walled composite I-beam.

Figure 3: Effect of load heights on the first load-frequency interaction curves with respect to the fiber angle change in the bottom flange of a simply supported composite beam under uniformly distributed load.

Figure 4: Effect of load heights on the first three load-frequency interaction curves with the fiber angle 0° in the bottom flange of a simply supported composite beam under uniformly distributed load.

Figure 5: Effect of load heights on the first three load-frequency interaction curves with the fiber angle 30° in the bottom flange of a simply supported composite beam under uniformly distributed load.

Figure 6: Effect of load heights on the first three load-frequency interaction curves with the fiber angle 60° in the bottom flange of a simply supported composite beam under uniformly distributed load.

Figure 7: The first four normal mode shapes of the flexural and torsional components with the fiber angle 30° in the bottom flange of a simply supported composite beam under combined axial compressive force ($\overline{N} = 0.5\overline{N}_{cr}$) and bending moment ($\overline{M} = 0.5\overline{M}_{cr}$).

Figure 8: The first three moment-frequency interaction curves with the fiber angle 30° in the bottom flange of a simply supported composite beam.

Figure 9: The first three moment-frequency interaction curves with the fiber angle 30° in the bottom flange of a simply supported composite beam under an axial compressive force ($\overline{N} = 0.5\overline{N}_{cr}$).

Figure 10: Effect of axial force on the first load-frequency interaction curves with fiber angles 30° and 60° in the bottom flange of a cantilever composite beam under point load at shear center of free end.

Figure 11: The first load-frequency interaction curves with respect to the axial compressive force change with fiber angles 30° and 60° in the bottom flange of a cantilever composite beam under point load at shear center of free end.

TABLE 1 Effect of axial force and bending moment on the first four natural frequencies with respect to the fiber angle change in the bottom flange of a simply supported composite beam.

| Fiber angle	$\overline{N}_{cr}$	$\overline{M}_{cr}$ ($\times 10^{-2}$)	Moment & Axial force	Present				Orthotropy			
				ω_1	ω_2	ω_3	ω_4	ω_{ya_1}	ω_{yb_1}	ω_{ya_2}	ω_{xx_1}
0	5.153	7.370	$\overline{M} = 0.5\overline{M}_{cr}$	2.914	6.204	18.657	19.830	2.914	6.204	18.657	19.830
30	2.771	4.895	$\overline{N} = 0.5\overline{N}_{cr}$	3.049	4.108	12.652	16.205	2.629	4.355	13.595	16.240
60	1.259	3.117	(compression)	2.050	3.655	5.990	12.317	1.836	3.353	6.019	14.596
90	1.112	2.905		1.895	3.674	5.450	11.146	1.695	3.360	5.453	14.523
0	5.153	7.370	$\overline{M} = 0.5\overline{M}_{cr}$	3.980	7.522	19.654	20.148	3.980	7.522	19.654	20.148
30	2.771	4.895	$\overline{N} = 0$	3.672	4.772	14.120	16.429	3.102	5.471	14.034	16.449
60	1.259	3.117	(no axial force)	2.650	3.712	7.014	13.492	2.148	4.027	6.850	14.703
90	1.112	2.905		2.448	3.721	6.422	12.270	2.021	3.945	6.268	14.617
0	5.153	7.370	$\overline{M} = 0.5\overline{M}_{cr}$	4.769	8.666	20.461	20.518	4.769	8.666	20.461	20.518
30	2.771	4.895	$\overline{N} = -0.5\overline{N}_{cr}$	4.165	5.551	15.214	16.677	3.781	6.240	14.697	16.656
60	1.259	3.117	(tension)	3.068	4.066	7.855	14.513	2.639	4.481	7.647	14.808
90	1.112	2.905		2.857	4.022	7.226	13.254	2.487	4.353	7.040	14.710
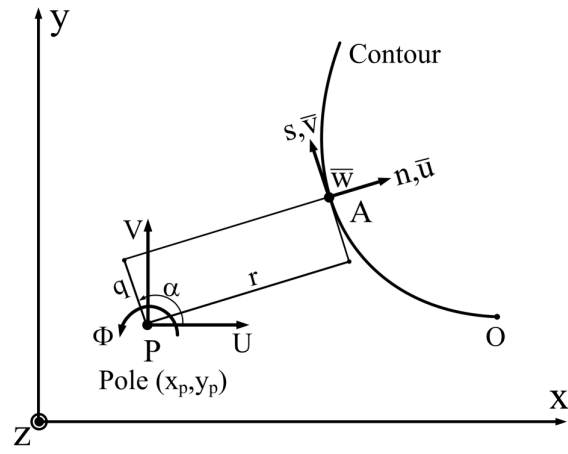
FIG. 1 Definition of coordinates in thin-walled open sections.
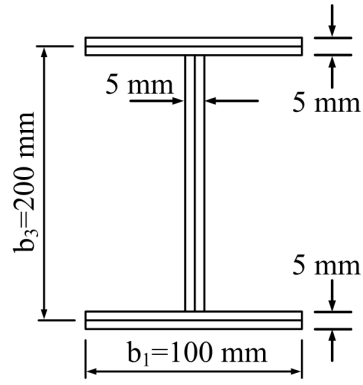
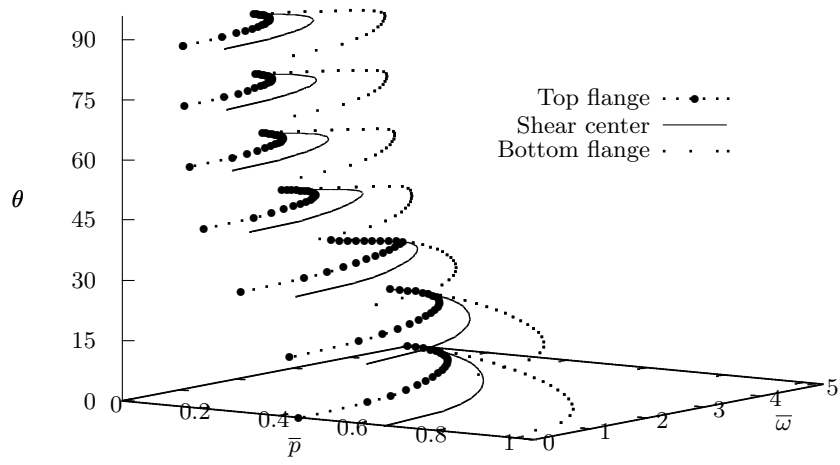FIG. 2 Geometry of thin-walled composite I-beam.

FIG. 3 Effect of load heights on the first load-frequency interaction curves with respect to the fiber angle change in the bottom flange of a simply supported composite beam under uniformly distributed load.
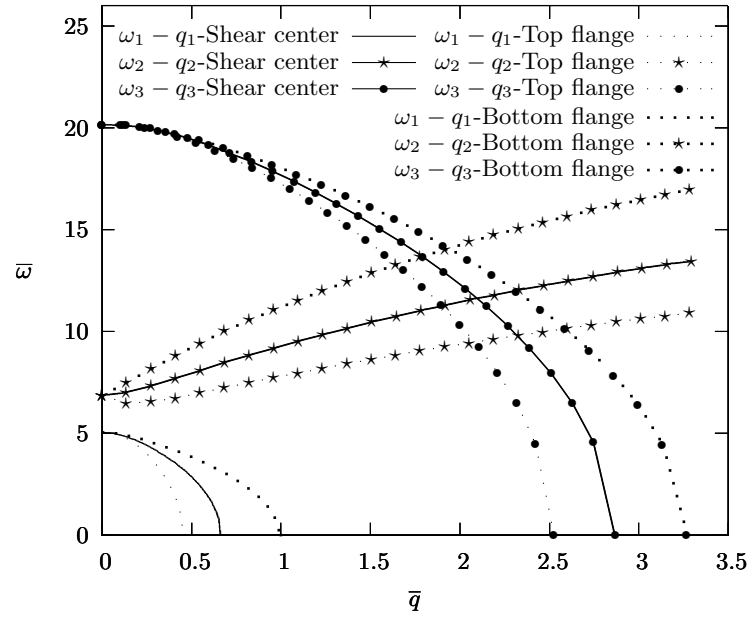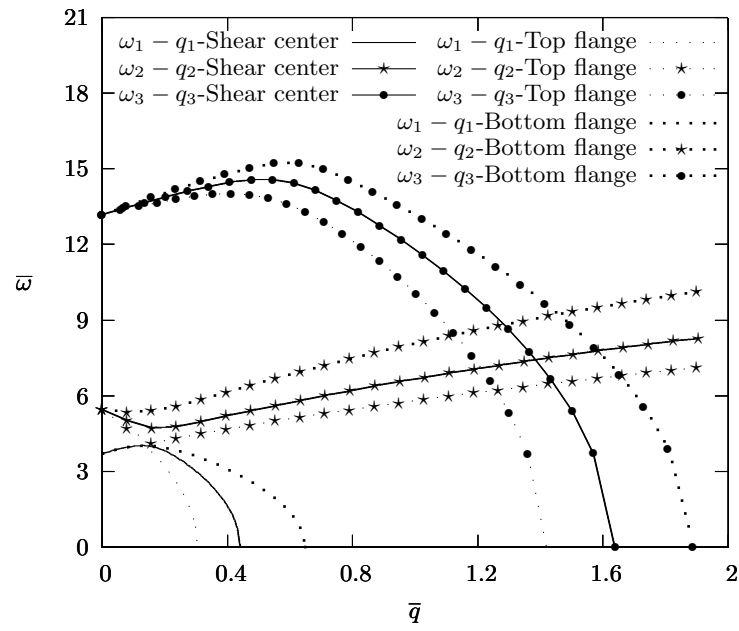
FIG. 4 Effect of load heights on the first three load-frequency interaction curves with the fiber angle $0°$ in the bottom flange of a simply supported composite beam under uniformly distributed load.
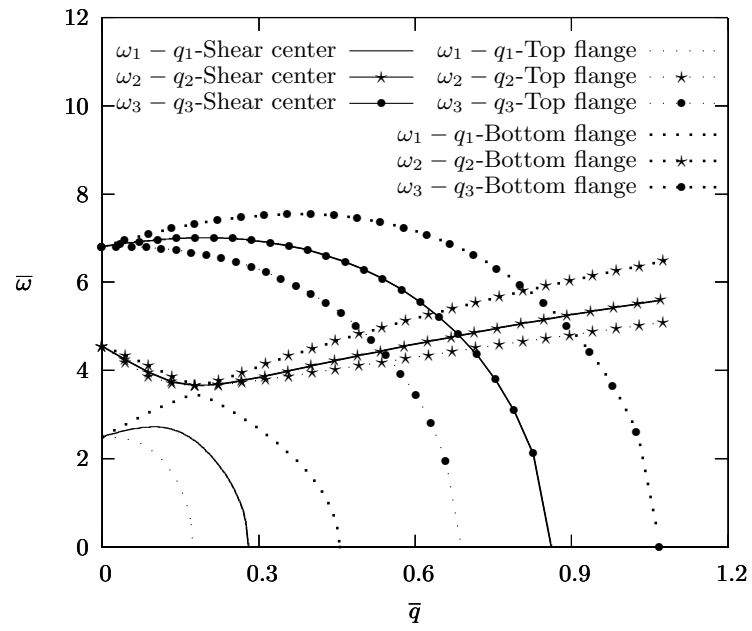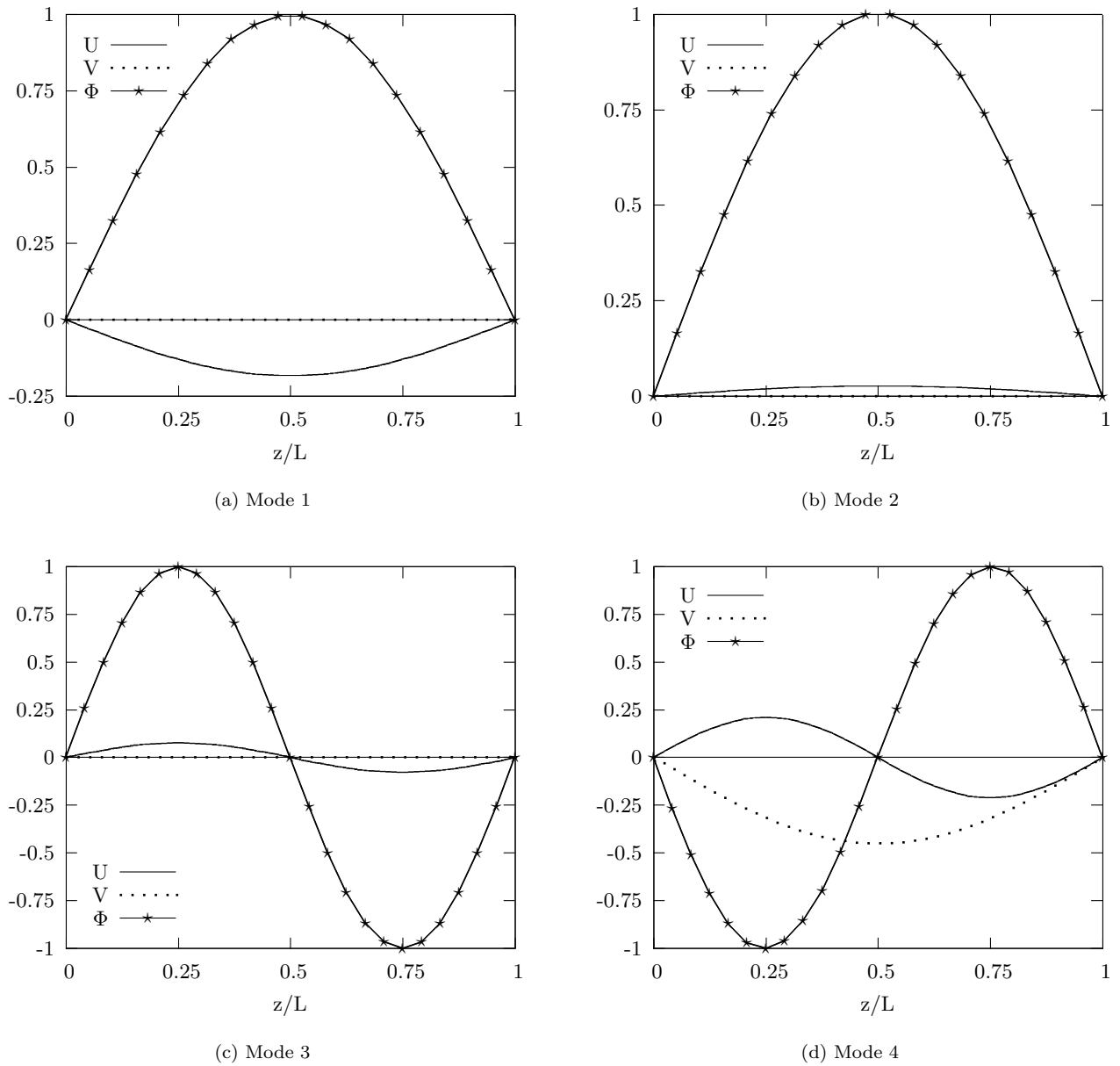
FIG. 5 Effect of load heights on the first three load-frequency interaction curves with the fiber angle $30°$ in the bottom flange of a simply supported composite beam under uniformly distributed load.
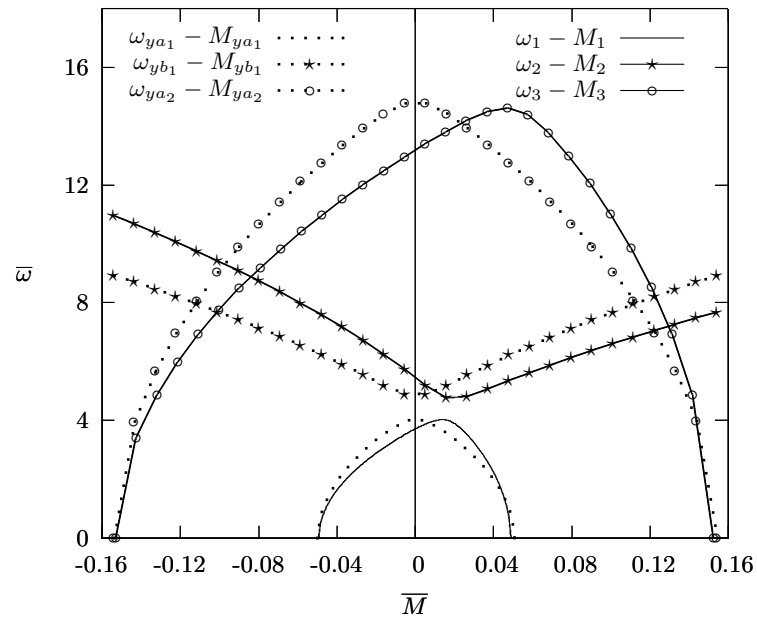
FIG. 6 Effect of load heights on the first three load-frequency interaction curves with the fiber angle 60° in the bottom flange of a simply supported composite beam under uniformly distributed load.

(a) Mode 1

(b) Mode 2

(c) Mode 3

(d) Mode 4

FIG. 7 The first four normal mode shapes of the flexural and torsional components with the fiber angle $30°$ in the bottom flange of a simply supported composite beam under combined axial compressive force ($\overline{N} = 0.5\overline{N}_{cr}$) and bending moment ($\overline{M} = 0.5\overline{M}_{cr}$).

FIG. 8 The first three moment-frequency interaction curves with the fiber angle $30°$ in the bottom flange of a simply supported composite beam.
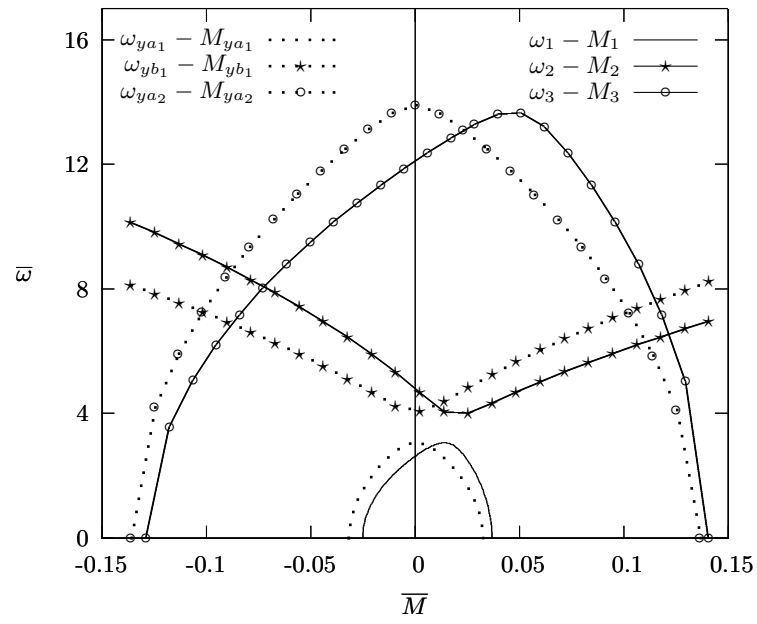
FIG. 9 The first three moment-frequency interaction curves with the fiber angle $30°$ in the bottom flange of a simply supported composite beam under an axial compressive force $(\overline{N} = 0.5\overline{N}_{cr})$.
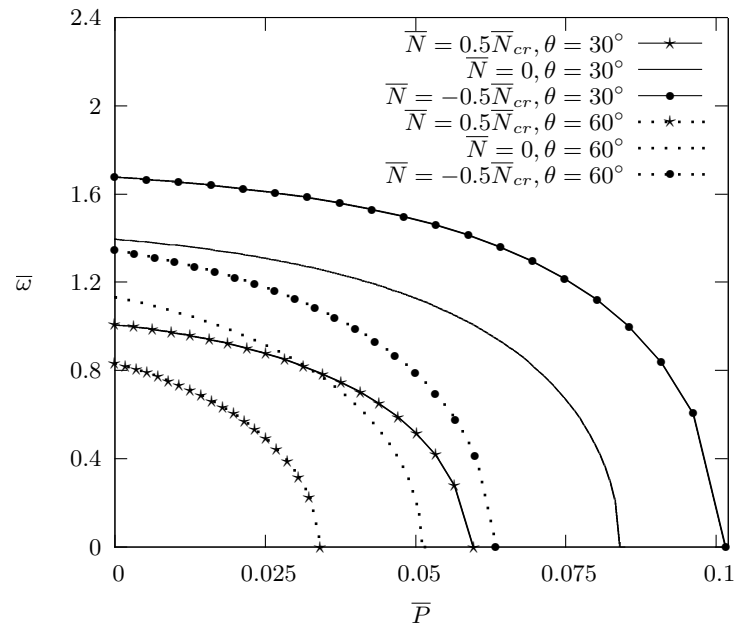
FIG. 10 Effect of axial force on the first load-frequency interaction curves with fiber angles $30°$ and $60°$ in the bottom flange of a cantilever composite beam under point load at shear center of free end.
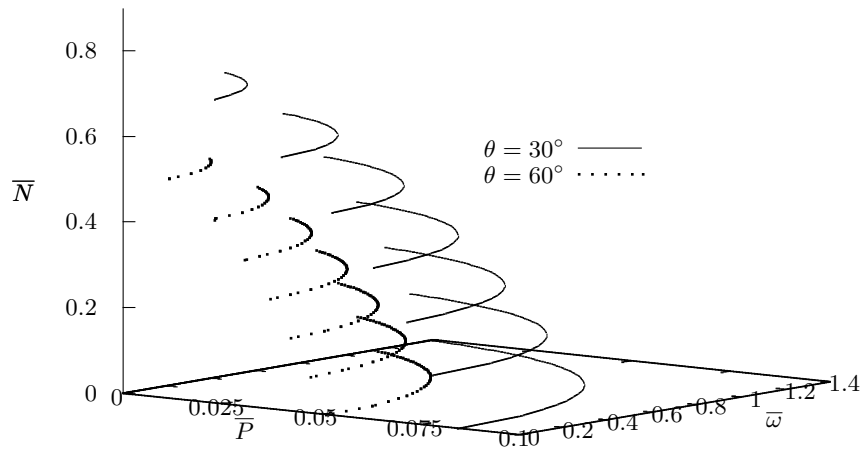
FIG. 11 The first load-frequency interaction curves with respect to the axial compressive force change with fiber angles $30°$ and $60°$ in the bottom flange of a cantilever composite beam under point load at shear center of free end.